

# Design a MIMO printed dipole antenna for 5G sub-band applications

Haider Saad Najim<sup>1</sup>, Mahmood Farhan Mosleh<sup>1</sup>, Raed A. Abd-Alhameed<sup>2</sup>

<sup>1</sup>Computer Techniques Engineering, Middle Technique University, Baghdad, Iraq

<sup>2</sup>Faculty of Engineering and Informatics, University of Bradford, Bradford, United Kingdom

## Article Info

### Article history:

Received Apr 8, 2022

Revised Jun 24, 2022

Accepted Jul 4, 2022

### Keywords:

5G

Omnidirectional radiation

Printed dipole antenna

Sub-6 GHz

## ABSTRACT

In this paper, a planar multiple input, multiple output (MIMO) dipole antenna for a future sub-6 GHz 5G application is proposed. The planar MIMO structure consists of 4 antenna elements with an overall size of  $150 \times 82 \times 1$  mm<sup>3</sup>. The single antenna element is characterized by a size of  $32.5 \times 33.7 \times 1$  mm<sup>3</sup> printed on an FR-4 dielectric substrate with  $\epsilon_r=4.4$  and  $\tan\delta=0.02$ . The suggested antenna structure exhibits good impedance bandwidth equal to 3.24 GHz starting from 3.3 to 6.6 GHz with an  $S_{11}$  value of less than -10 dB ( $S_{11} \leq -10$  dB) with antenna gain varying from 5.2 up to 7.05 dB in the entire band, which covers all the sub-6 GHz frequency band of the 5G application. Good isolation is achieved between the MIMO elements due to low surface waves inside the MIMO antenna substrate. The radiation of the MIMO antenna structure can be manipulated and many beam-types can be achieved as desired. The high-frequency structure simulator (HFSS) software package is used to design and simulate the proposed structure, while the CST MWS is used to validate the results.

*This is an open access article under the [CC BY-SA](https://creativecommons.org/licenses/by-sa/4.0/) license.*



## Corresponding Author:

Haider Saad Najim

Computer Techniques Engineering, Middle Technique University

Baghdad, Iraq

E-mail: [haidersaadct@mtu.edu.iq](mailto:haidersaadct@mtu.edu.iq)

## 1. INTRODUCTION

With a wide development in the wireless communications system and a large amount of devices that require a wideband of operating frequencies, the fifth-generation (5G) system has been occurred to increase the capacity, speed, energy efficiency, and reliability of the network [1]-[7]. Due to that development in the network, the needs for wide-bandwidth, light weight, low-profile, and small size antennas with stable radiation and good characteristics are in increasing [8]-[11]. Conventional printed antennas, on the other hand, may not meet such criteria as wideband, high-speed data transmission; steady unidirectional emission over a broad frequency range; and high gain [10], [12]-[14].

Due to its high gain and unidirectional radiation patterns, the traditional Yagi antenna is frequently employed in wireless communication networks [15]-[22]. The traditional Yagi antenna has a narrow impedance bandwidth with a big size and can't be integrated with a circuit board, which limits its use in some applications [23]. A Yagi antenna is composed of three primary components: the reflector, the driving elements, and the director [24]. In 1991, Huang and Densmore invented the planar microstrip Yagi antenna as a hybrid of Yagi and microstrip antennas, which has many of the properties of a Yagi antenna, including high gain, steady radiation, cheap cost, and simplicity of production and circuit board integration [25]. Many techniques are used to develop and enhance the planar Yagi antenna structure performance. To obtain a broad

impedance bandwidth, a Microstrip to Slotline feeding approach is presented, and the measured result is found to be approximately 46% [26].

In this work, a multiple input, multiple output (MIMO) planar printed dipole antenna is proposed for Sub-6GHz 5G mobile applications. The MIMO structure size is  $150 \times 82 \text{ mm}^2$ . A microstrip to slotline transition technique is used as an antenna feedline to avoid high cross-polarization. A tapered slot technique is suggested as the dipole driver of a printed dipole antenna. Such drivers allow the proposed antenna to work at a considerable bandwidth with good performance, this makes it an excellent choice for 5G applications.. Four antenna elements are used in the MIMO structure. Each antenna element is placed in a corner to achieve omni-directional radiation. In order to design and simulate the suggested structure, the high-frequency structure simulator (HFSS) software package is employed, and the CST MWS is used to verify the results.

**2. ANTENNA DESIGN METHOD**

**2.1. Single antenna element**

The suggested antenna structure based on the printed dipole antenna is presented in Figure 1. The antenna structure is printed on an FR-4 dielectric substrate with  $\epsilon_r=4.4$ , and  $\tan\delta=0.02$ . The antenna dimensions are  $32.5 \times 33.7 \text{ mm}^2$  with a substrate thickness of 1mm. On the bottom face of the FR-4 substrate is printed the antenna feedline. The feedline technique that is used in the proposed antenna is the microstrip to slotline transition type with impedance of  $50 \Omega$ . A square-shaped stub with dimensions of  $4 \times 4 \text{ mm}^2$  is located at the end of the microstrip transmission line. Such a stub is used for more impedance matching.

The patch layer of the suggested antenna is printed on the top face of the FR-4 substrate. As seen in Figure 1, the patch structure is comprised of a reflector, drivers with a flare shape, and a director. The antenna drivers are characterized by a flare-shape with a tapered slot curve. The taper slot technique is used in the proposed antenna due to the advantages presented by wide impedance bandwidth, high gain, and symmetrical radiation pattern. Finally, the other geometrical details are presented in Table 1.

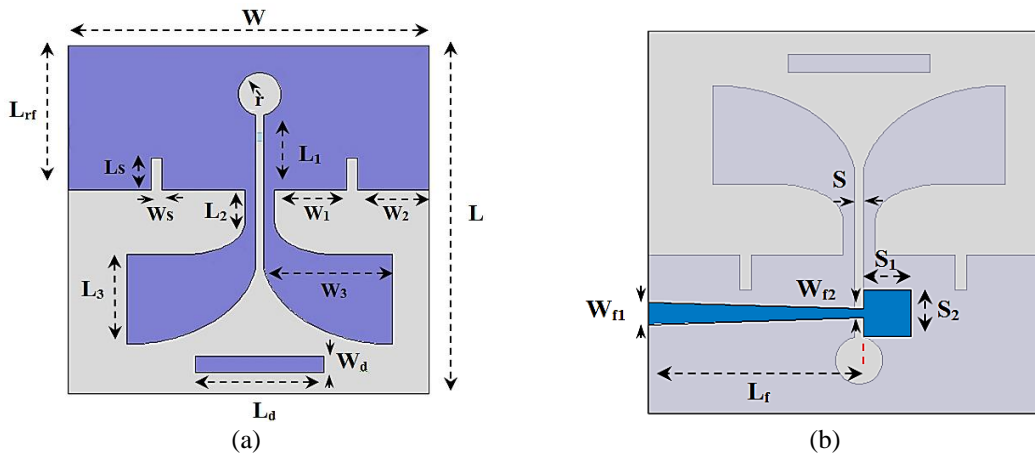


Figure 1. The geometrical shape of the suggested printed dipole antenna (a) top view and (b) bottom view

Table 1. The geometrical details of the suggested printed dipole antenna (all measurements in mm).

Parameter	Value	Parameter	Value	Parameter	Value	Parameter	Value
L	32.5	L <sub>s</sub>	3	L <sub>3</sub>	8.4	W <sub>f2</sub>	0.8
W	33.7	W <sub>s</sub>	1	W <sub>3</sub>	12	L <sub>r</sub>	18.3
L <sub>rf</sub>	13.5	L <sub>2</sub>	3	L <sub>d</sub>	12	S	0.8
r	1	W <sub>1</sub>	6.7	W <sub>d</sub>	1.5	S <sub>1</sub>	4
L <sub>1</sub>	7	W <sub>2</sub>	6.7	W <sub>f1</sub>	1.9	S <sub>2</sub>	4

In Figure 2, the antenna development steps of the proposed antenna structure are presented as Ant.1, Ant.2, Ant.3, and Ant.4. At the top of the dielectric substrate, the reflector and driver are mounted, while at the bottom, there is a feedline. The antenna feedline is kept constant for all the antenna models. Initially, Ant.1 was designed. It's a conventional printed dipole antenna with two straight-line drivers. Each driver is characterized by a size of  $12 \times 1 \text{ mm}^2$ .

In the second step of the proposed antenna development, the antenna driver elements are modified to the linear tapered slot as seen in Figure 2. The linear tapered slot technique is used to enhance the antenna performance due to the linear slot transition. The tapered slot gives linear variation in the opening of the slot curved. This variation in the slot curve gives more antenna impedance variation. As there more impedance variation there is more operating frequency. At the end of the slot, the impedance is closed to the free-space impedance and as a result the radiation is happened. In Ant.3, the linear slot curve is improved to an exponential slot curve to give a smooth slot transition and, as a result, more variation in the opening of the slot curve. Finally, in Ant.4, a single director element is added to the antenna structure for more antenna performance enhancement.

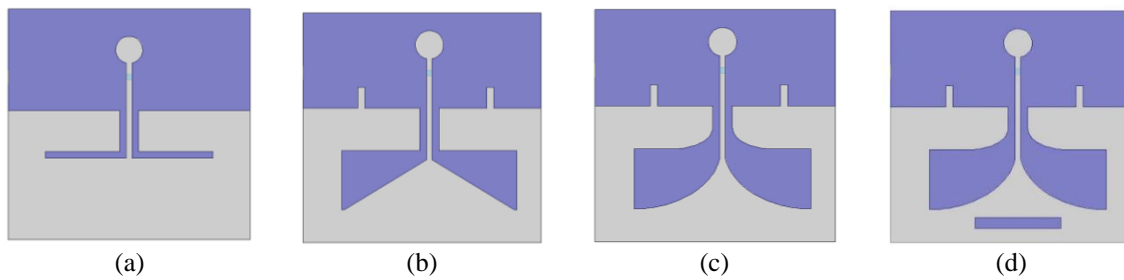


Figure 2. The suggested planned dipole antenna's design steps: (a) Ant.1, (b) Ant.2, (c) Ant.3, and (d) Ant.4

**2.2. MIMO antenna system**

After completing the designing process of the suggested planar dipole antenna, optimum design is achieved, and a MIMO antenna system is designed and presented in Figure 3. Four antenna element structures are used and printed on the dielectric substrate of FR-4 material. The MIMO antenna's overall dimensions are 150×82 mm<sup>2</sup> with a substrate thickness of 1 mm. Due to the proposed planar dipole antenna characteristic of the endfire radiation pattern, each antenna element is placed in one corner of the substrate toward one of the four directions. Such an arrangement is used to cover all four directions in order to achieve an omnidirectional radiation pattern. The MIMO geometrical details are presented in Table 2.

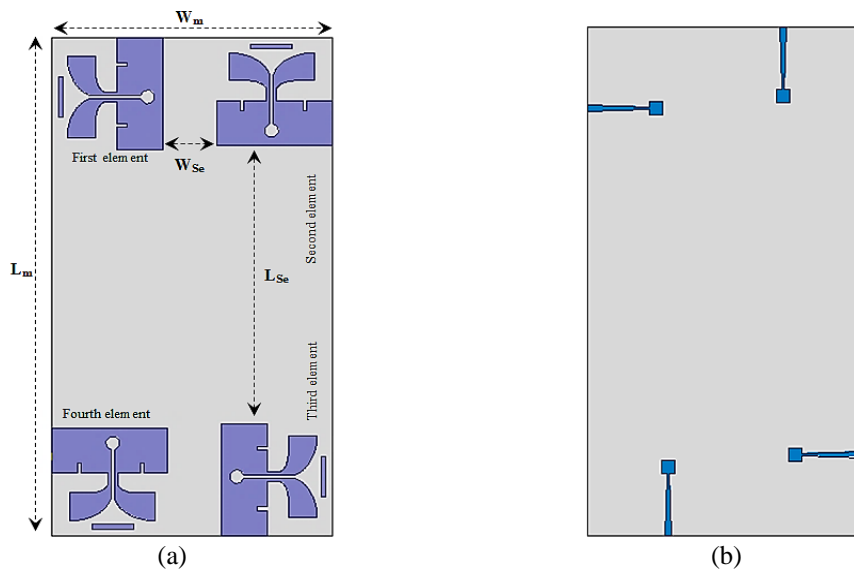


Figure 3. The geometrical shape of the printed Dipole MIMO antenna (a) top view and (b) back view

Table 2. Geometrical details of MIMO antenna system (all measurements in mm)

Parameter	Value	Parameter	Value
Lm	150	L <sub>se</sub>	83.7
Wm	82	W <sub>se</sub>	15.7

### 3. RESULTS AND DISCUSSIONS

#### 3.1. Single antenna element

After completing the designing process of the suggested antenna structure, the suggested antenna is simulated and analyzed inside the HFSS environment. Firstly, the reflection coefficient of the proposed antenna in terms of  $S_{11}$  is calculated and presented in Figure 4. It's found that the simulated result shows and gives a wideband of impedance bandwidth. The bandwidth is found to be equal to 3.24 GHz starting from 3.3 to 6.6 GHz with an  $S_{11}$  value of less than -10dB ( $S_{11} \leq -10$  dB) in the entire band, which covers all the sub-6 GHz frequency band of the 5G application. The best result with the lowest  $S_{11}$  value is found at a frequency of 6 GHz, with an  $S_{11}$  value equal to -40 dB.

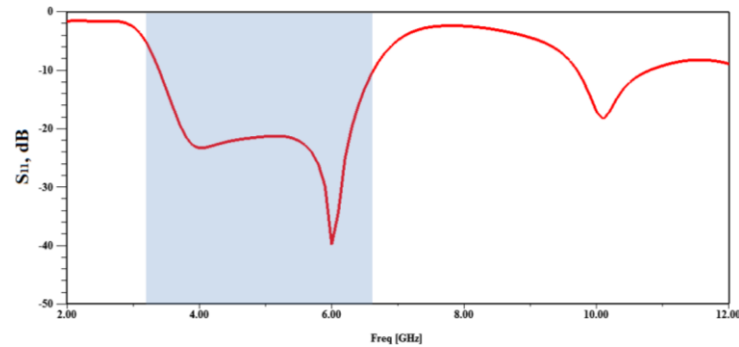


Figure 4. Return loss ( $S_{11}$ ) in dB of the suggested antenna design

In Figure 5, the  $S_{11}$  spectra of all antenna models are presented as Ant.1, Ant.2, Ant.3, and Ant.4. The first antenna model, Ant.1, showed an impedance bandwidth equal to 1.58 GHz starting from 3.6 to 5.19 GHz with the lowest  $S_{11}$  value equal to -34.7 dB at the resonant frequency of 4GHz. The Ant.2 showed an impedance bandwidth starting from 3.25 to 4.66 GHz with an  $S_{11}$  value  $\leq -10$  dB, while the lowest  $S_{11}$  value of the Ant.2 was found to be equal to -26.5 dB at the resonant frequency of 3.69 GHz. The third antenna model that was presented by Ant.3 showed a better result compared with the other previous models, where it showed an impedance bandwidth equal to 2.43 GHz starting from 3.36 to 5.79 GHz with an  $S_{11}$  value  $\leq -10$  dB, and the lowest  $S_{11}$  value was found to be equal to -37.1 dB at the resonant frequency of 3.9 GHz. Finally, the last antenna model that was presented by Ant.4 showed the best results and wider impedance bandwidth compared with all the previous models, which provided a bandwidth of equal to equal to 3.24 GHz starting from 3.3 to 6.6 GHz with an  $S_{11}$  value of less than -10 dB ( $S_{11} \leq -10$  dB) in the entire band, which covers all the sub-6 GHz frequency band of the 5G application. The best result with the lowest  $S_{11}$  value is found at 6 GHz, with an  $S_{11}$  value equal to -40 dB.

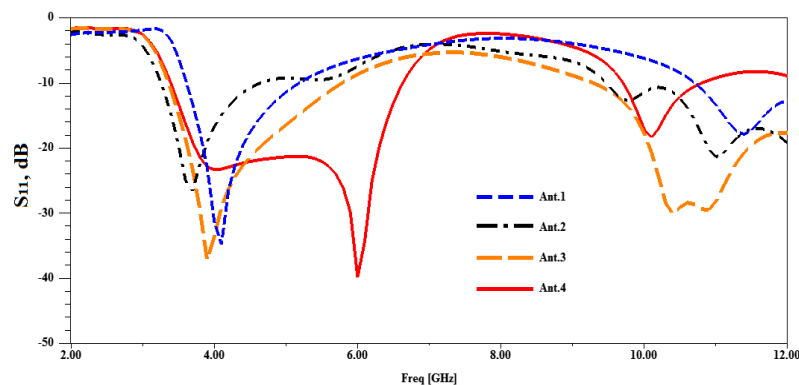


Figure 5. Return loss ( $S_{11}$ ) in dB of the all antenna design models

Next, the gain of the suggested planar dipole antenna structure is evaluated. The obtained result indicates that the gain of the suggested antenna structure varies from 5.2 up to 7.05 dB in the entire band of the operating frequency, as seen in Figure 6. The gain spectra of the other antenna models are evaluated and presented in Figure 7. From the evaluated results, the gain of the first antenna model is found to vary from 4.5 up to 5 dB in the entire band, while the gain of the second antenna model is found to vary from 4.83 up to 5.13 dB. Next, the gain of the third antenna model is evaluated, where it's found to vary from 5 to 5.41 dB in the entire band. Finally, the gain of the last antenna model is evaluated, and it's found that the last model has a higher gain compared with the other three models, where the gain of the last model is found to vary from 5.2 up to 7.05 dB in the entire band. In Figure 8, the axial ratio of all the antenna models is evaluated. It's found that all antenna models show linear polarization behavior in the entire band of operating frequency with a value greater than 3 dB for all antenna models.

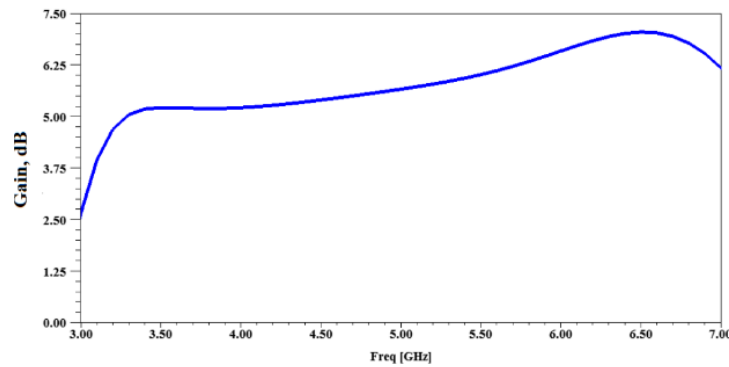


Figure 6. Gain vs Frequency (in dB) of the suggested antenna design

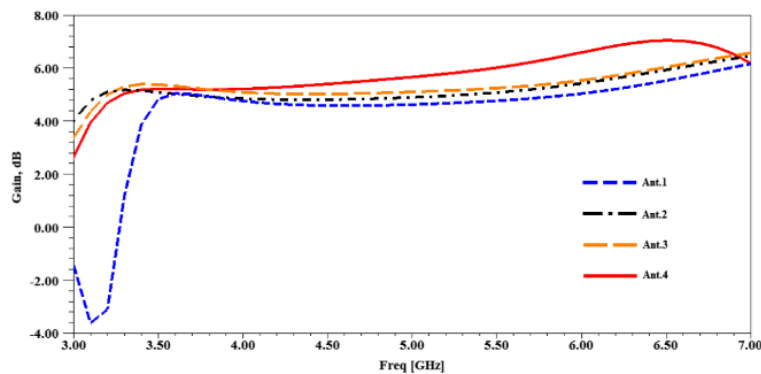


Figure 7. Gain comparison between the all antenna models

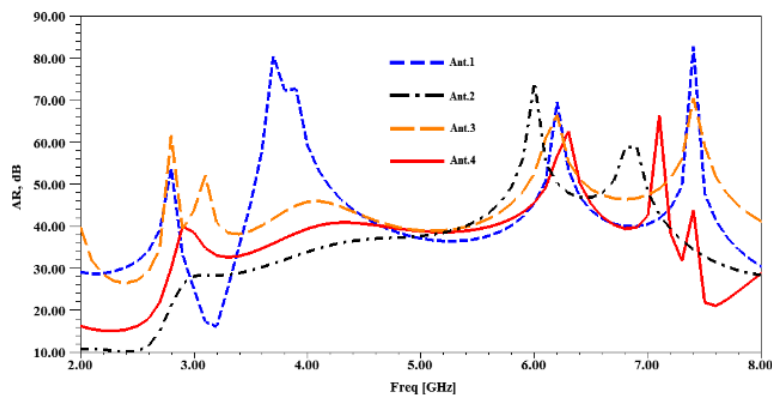


Figure 8. Axial ratio comparison between all antenna models

For more accurate results, the CST MWS is used to design and simulate the proposed planar dipole antenna structure. As seen in Figure 9, an excellent agreement is found between both software in terms of  $S_{11}$ . Both software's results cover the entire sub-6GHz band for 5G applications. In Figure 10, the current distribution of the suggested antenna is evaluated and the behavior is studied. It's noticed that the current in the radiating wings is flowing from the bottom, starting from the beginning of the flare curve to the front of the upper wing, end of the flare curve. This behavior of the current will create an E-field parallel to the antenna, and as a result, endfire radiation will be achieved. The 2D-radiation patterns of the optimum planar dipole antenna design are evaluated in terms of X.Y-Plane and X.Z-Plane at different operating frequencies, as seen in Figure 11. From both results, it's found that the antenna is characterized by stable radiation pattern based on end-fire type in the entire band of operating frequency due to the current behavior in the radiating wings.

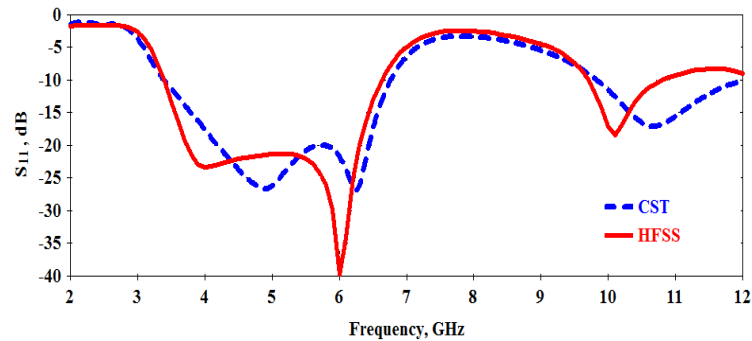


Figure 9. Return loss comparison of the planar dipole antenna.

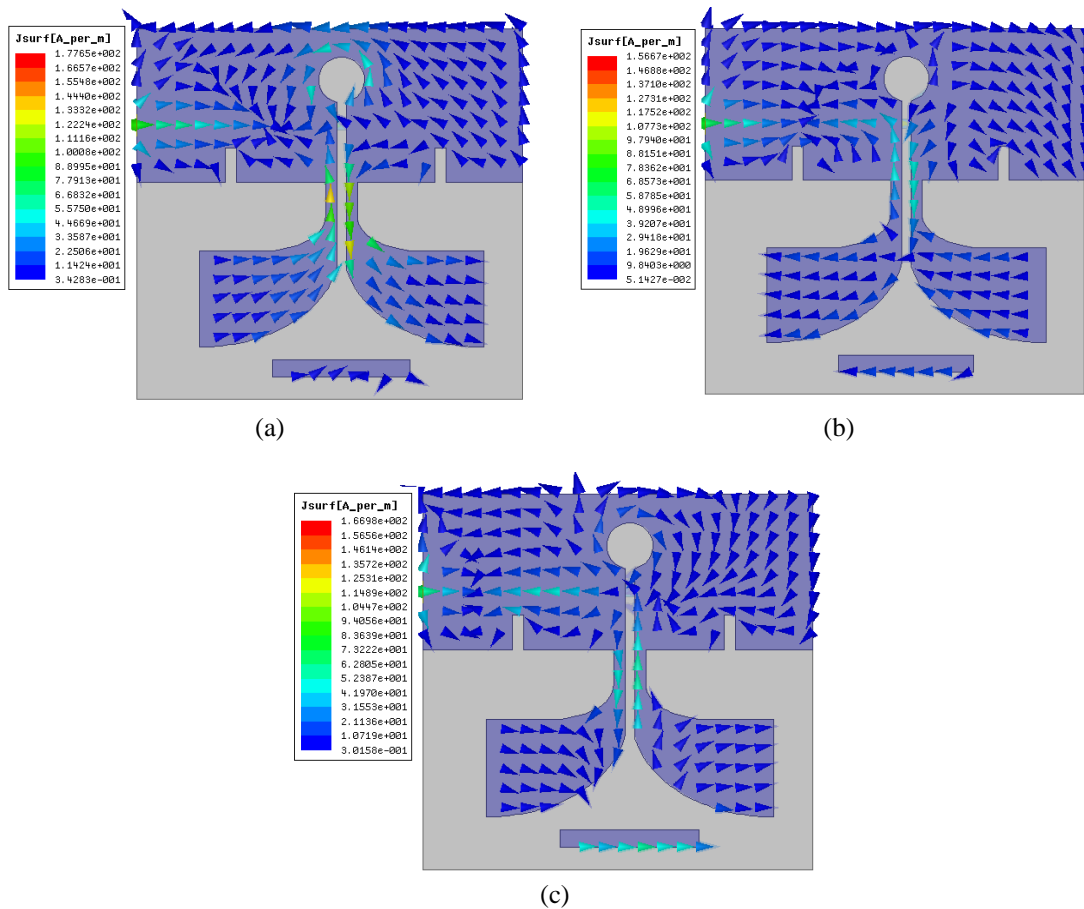


Figure 10. Distributions of current in the planar dipole antenna (a) 3.4 GHz, (b) 5 GHz, and (c) 6.6 GHz

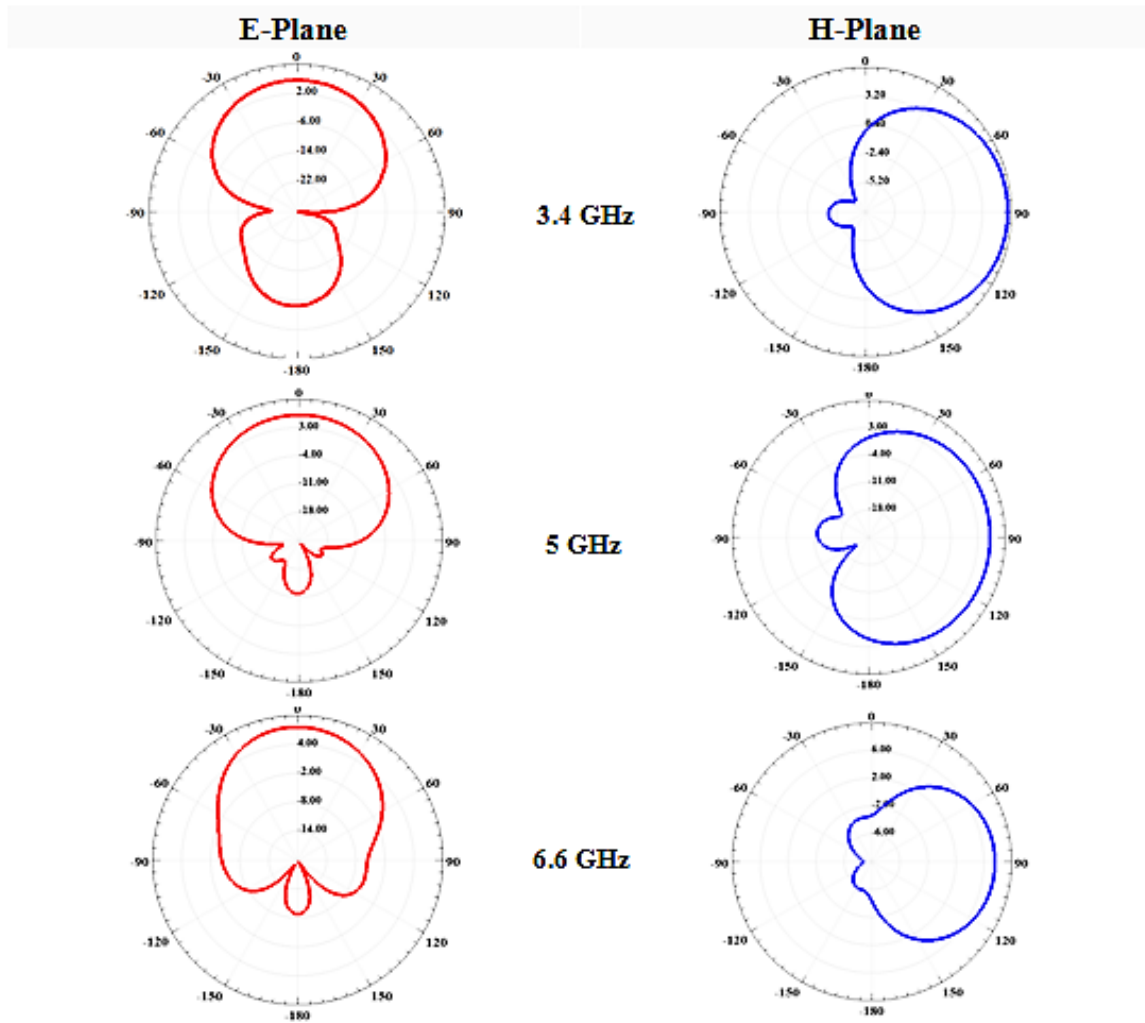


Figure 11. E and H fields of the planar dipole antenna at different frequency band

### 3.2. MIMO antenna system

After completing the design and simulation process of the proposed antenna structure, the MIMO antenna structure is designed and simulated inside the HFSS environment. Firstly, the reflection coefficients,  $S_{ii}$ , of the MIMO antenna design in terms of  $S_{11}$ ,  $S_{22}$ ,  $S_{33}$ , and  $S_{44}$ , are evaluated and presented in Figure 12. It's found that the simulated results show excellent agreement and provide a wideband of impedance bandwidth. The bandwidth is found to be equal to 3.24 GHz starting from 3.3 to 6.6 GHz with values less than -10 dB ( $S_{ii} \leq -10$  dB) in the entire band, which covers all the sub-6 GHz frequency band of the 5G application.

Next, the transmission coefficients,  $S_{ij}$ , of the each two successive elements in the MIMO antenna structure are evaluated and presented in Figure 13 in term of  $S_{12}$ ,  $S_{23}$ ,  $S_{34}$ , and  $S_{41}$ . Its notice a good isolation is found between the MIMO elements due to low surface waves inside the MIMO antenna substrate. The isolation value between the first and second antenna elements ( $S_{12}$ ), and between the third and fourth antenna elements ( $S_{34}$ ) is found less than -23 dB in the entire band which is varying from -24 to -43 dB. While the isolation value between the second and third antenna elements ( $S_{23}$ ), and between the fourth and first antenna elements ( $S_{41}$ ) is found less than -42 dB in the entire band which varies from -42.5 to -51 dB. As illustrated in Figure 3, the distance between the first and second antenna elements, and between the third and fourth antenna elements, is less than the distance between the second and third antenna elements, and between the fourth and first antenna elements, so that the isolation is lower between the elements that are closer to each other and higher between the elements that are farther from each other.

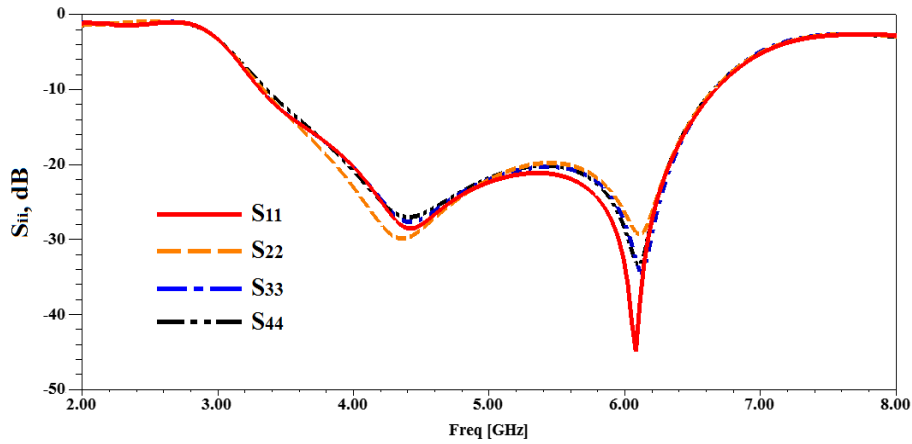


Figure 12. Return loss ( $S_{11}$ ,  $S_{22}$ ,  $S_{33}$ , and  $S_{44}$ ) in dB for the designed MIMO elements

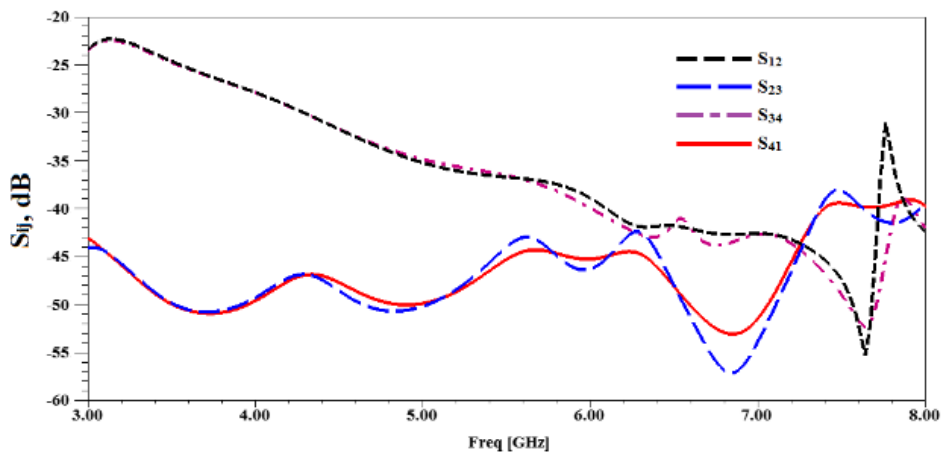


Figure 13. The mutual coupling ( $S_{12}$ ,  $S_{23}$ ,  $S_{34}$ , and  $S_{41}$ ) in dB between the designed MIMO elements

In Figure 14, the 3D-radiation patterns of the MIMO antenna structure are evaluated and presented for each port. Moreover, the 3D-radiation patterns of the MIMO antenna structure for all ports are presented in Figure 15. Additionally, as seen in Figure 16, the 2D-radiation pattern is analyzed in terms of the E-Plane and H-Plane at various operating frequencies. Due to the stable radiation pattern based on end-fire type, the MIMO antenna's radiation may be controlled and a variety of beam types can be created.

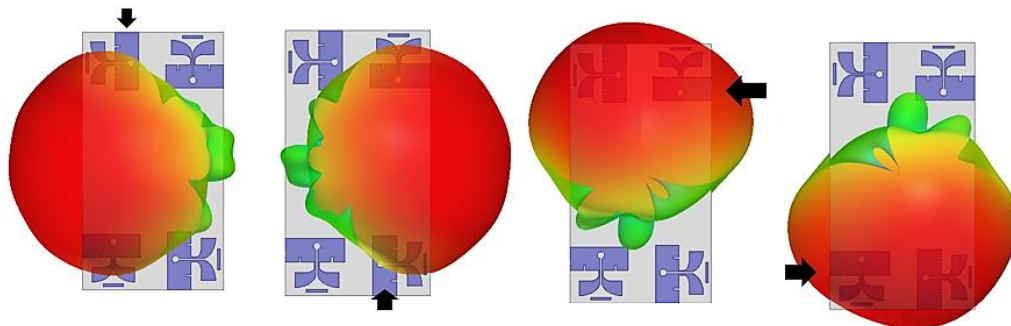


Figure 14. The MIMO antenna structure's 3D radiation patterns for each ports



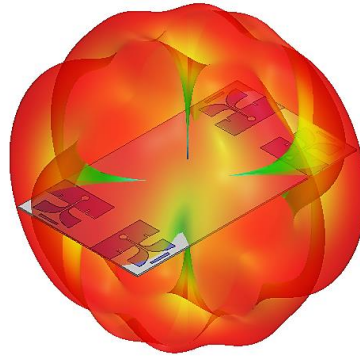


Figure 15. The MIMO antenna structure's 3D radiation patterns for all ports

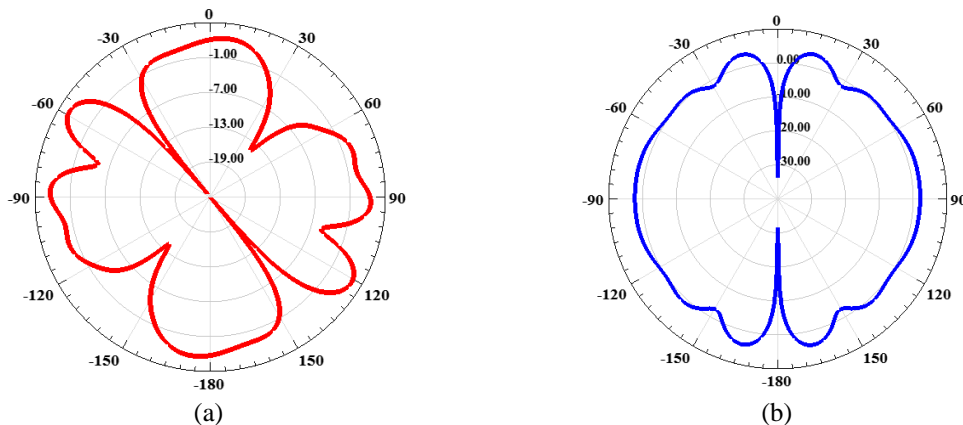


Figure 16. 2D-radiation pattern in terms of E-Plane and H-Plane of the proposed antenna (a) XY-Plane and (b) XZ-Plane

Figure 17 depicts the envelope correlation coefficient (ECC), an essential statistic used to assess the correlation between MIMO components. The ECC can be determined by using the following (1):

$$\rho_{eij} = \frac{|s_{ii}^* s_{ij} + s_{ji}^* s_{jj}|^2}{(1 - |s_{ii}|^2 - |s_{ij}|^2)(1 - |s_{ji}|^2 - |s_{jj}|^2)} \tag{1}$$

where  $\rho$  is the ECC and  $S_{ij}$  are the MIMO system's S-parameters. The lower correlation means less overlap between the two beam patterns [27]. As seen in Figure 17, the ECC is smallest than 0.005 across the entire band, which is significantly less than the standard value (0.5) [28].

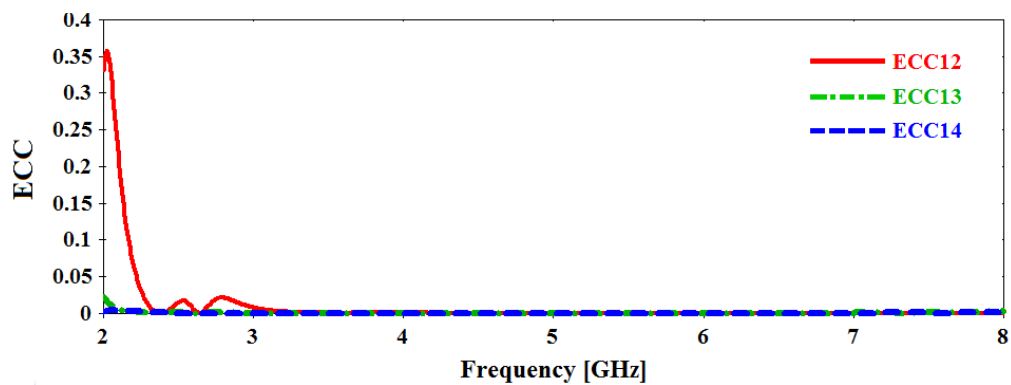


Figure 17. The ECC of the suggested MIMO system

Diversity Gain (DG), which may be determined using the following formula (2), is another important performance measure for antennas [29]:

$$DG = 10\sqrt{1 - |\rho_{eij}|^2} \quad (2)$$

as illustrated in Figure 18, the DG approaches 10 dB for all ports, which is an accepted value where this parameter must be (>9 dB) according to [30]. As indicated in Table 3, the suggested MIMO antenna design is compared to previous research on a variety of features.

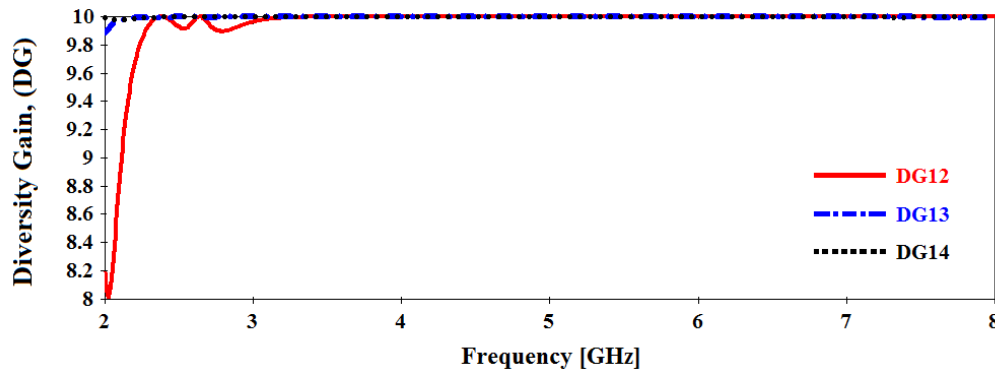


Figure 18. The DG of the suggested MIMO system

Table 3. Comparing the suggested design of the MIMO system to that of previous studies

References	No. of Ports	Antenna size (mm <sup>2</sup> )	Operating Frequency (GHz)	Bandwidth (GHz)	Isolation (dB)	Diversity gain (dB)	ECC
[31]	8	124×74	3.3–3.6	0.3	<-15	NA	<0.15
[32]	8	139×67	5.81–6.66	0.85	<-15	>9.995	<0.01
[33]	4	115×65	3.5–5.9	2.4	<-20	>9.985	<0.005
[34]	6	150×75	2.38-2.72/3.19–3.84	0.34/0.65	<-15	>9	<0.17
[35]	4	150×75	3.21–3.81	0.6	<-10	>9.6	<0.02
Proposed	4	150×82	3.3–6.6	3.24	<-23	>9.999	<0.005

#### 4. CONCLUSION





A planar MIMO dipole antenna for a future sub-6 GHz 5G application has been suggested in this paper. The planar MIMO structure includes four antenna elements with an overall size of 150×82×1 mm<sup>3</sup>. The impedance bandwidth of the suggested structure is found starting from 3.3 to 6.6GHz with gain varying from 5.2 dB up to 7.05 dB in the entire band. Moreover, good isolation is found between the MIMO elements. Due to the antennas arrangement in the MIMO structure, the radiation can be manipulated and many beam-types can be achieved. The suggested structure is designed and simulated by using the HFSS software, while the results are validated by using the CST MWS.

#### REFERENCES





- [1] W. Zeng, S. Qi, L. Liu, and Y. Yao, "Research on laser-generated Rayleigh waves with angled surface crack by finite element method," *Optik*, vol. 181, pp. 57-62, 2019, doi: 10.1016/j.ijleo.2018.11.105.
- [2] Z. A. A. Hassain, A. R. Azeez, M. M. Ali, and T. A. Elwi, "A modified compact bi-directional UWB tapered slot antenna with double band-notch characteristics," *Advanced Electromagnetics*, vol. 8, no. 4, 2019, doi: 10.7716/aem.v8i4.1130.
- [3] M. G. Kachhavay and A. PThakare, "5G technology-evolution and revolution," *International Journal of Computer Science and Mobile Computing*, vol. 3, no. 3, pp. 1080-1087, 2014.
- [4] M. D. Hill, D. B. Cruickshank, and I. A. MacFarlane, "Perspective on ceramic materials for 5G wireless communication systems," in *Applied Physics Letters*, vol. 118, no. 12, p. 120501, 2021, doi: 10.1063/5.0036058.
- [5] Y. Wu, X. Gao, S. Zhou, W. Yang, Y. Polyanskiy, and G. Caire, "Massive access for future wireless communication systems," *IEEE Wireless Communications*, vol. 27, no. 4, pp. 148-156, August 2020, doi: 10.1109/MWC.001.1900494.
- [6] O. A. Shareef, A. M. A. Sabaawi, K. S. Muttair, M. F. Mosleh, and M. B. Almashhdany, "Design of multi-band millimeter wave antenna for 5G smartphones," *Indonesian Journal of Electrical Engineering and Computer Science*, vol. 25, no. 1, pp. 382-387, 2022, doi: 10.11591/ijeecs.v25.i1.pp382-387.

- [7] A. Ahad, M. Tahir, M. A. Sheikh, K. I. Ahmed, A. Mughees, and A. Numani, "Technologies trend towards 5g network for smart health-care using iot: A review," *Sensors*, vol. 20, no. 14, p. 4047, 2020, doi: 10.3390/s20144047.
- [8] W. X. Liu, Y. Z. Yin, W. L. Xu, and S. L. Zuo, "Compact open-slot antenna with bandwidth enhancement," *IEEE Antennas and Wireless Propagation Letters*, vol. 10, pp. 850-853, 2011, doi: 10.1109/LAWP.2011.2165197.
- [9] L. Ge and K. M. Luk, "A wideband magneto-electric dipole antenna," *IEEE Transactions on Antennas and Propagation*, vol. 60, no. 11, pp. 4987-4991, Nov. 2012, doi: 10.1109/TAP.2012.2207689.
- [10] S. Wang, Q. Wu, and D. Su, "A novel reversed t-match antenna with compact size and low profile for ultrawideband applications," *IEEE Transactions on Antennas and Propagation*, vol. 60, no. 10, pp. 4933-4937, Oct. 2012, doi: 10.1109/TAP.2012.2207360.
- [11] D. Nagaraju and N. P. Gupta, "Design and Simulation of a Compact 5.4GHz H-shaped slot antenna for RF energy harvesting systems," in *IOP Conference Series: Materials Science and Engineering*, vol. 1033, p. 012031, 2021, doi: 10.1088/1757-899X/1033/1/012031.
- [12] T. T. Thai, G. R. DeJean, and M. M. Tentzeris, "Design and development of a novel compact soft-surface structure for the front-to-back ratio improvement and size reduction of a microstrip Yagi Array Antenna," *2007 IEEE Antennas and Propagation Society International Symposium*, 2007, pp. 1381-1384, doi: 10.1109/APS.2007.4395761.
- [13] T. Abeesh and M. Jayakumar, "Design and studies on dielectric resonator on-chip antennas for millimeter wave wireless applications," in *2011 - International Conference on Signal Processing, Communication, Computing and Networking Technologies, ICSCCN-2011*, 2011, pp. 322-325, doi: 10.1109/ICSCCN.2011.6024568.
- [14] K. E. Kedze and I. Park, "Silver nanoflake printed flexible composite broadband dipole antenna," in *ICEIC 2019 - International Conference on Electronics, Information, and Communication*, 2019, pp. 1-3, doi: 10.23919/ELINFOCOM.2019.8706379.
- [15] S. Lim and H. Ling, "Design of a closely spaced, folded Yagi antenna," *IEEE Antennas and Wireless Propagation Letters*, vol. 5, pp. 302-305, 2006, doi: 10.1109/LAWP.2006.878892.
- [16] D. Z. Kim, S. Y. Park, W. S. Jeong, M. Q. Lee, and J. W. Yu, "A small and slim printed yagi antenna for mobile applications," *2008 Asia-Pacific Microwave Conference*, 2008, pp. 1-4, doi: 10.1109/APMC.2008.4958413.
- [17] E. Ávila-Navarro, J. A. Carrasco, and C. Reig, "Design of Yagi-like printed antennas for wlan applications," *Microwave and Optical Technology Letters*, vol. 49, no. 9, pp. 2174-2178, pp. 2174-2178, 2007, doi: 10.1002/mop.22655.
- [18] N. Kaneda, W. R. Deal, Y. Qian, R. Waterhouse, and T. Itoh, "A broad-band planar quasi-Yagi antenna," *IEEE Transactions on Antennas and Propagation*, vol. 50, no. 8, pp. 1158-1160, Aug. 2002, doi: 10.1109/TAP.2002.801299.
- [19] P. Y. Qin, A. R. Weily, Y. J. Guo, T. S. Bird, and C. H. Liang, "Frequency reconfigurable quasi-Yagi folded dipole antenna," *IEEE Transactions on Antennas and Propagation*, vol. 58, no. 8, pp. 2742-2747, Aug. 2010, doi: 10.1109/TAP.2010.2050455.
- [20] Y. Cai, Y. J. Guo, and P. Y. Qin, "Frequency switchable printed Yagi-Uda dipole sub-array for base station antennas," *IEEE Transactions on Antennas and Propagation*, vol. 60, no. 3, pp. 1639-1642, March 2012, doi: 10.1109/TAP.2011.2180337.
- [21] W. R. Deal, N. Kaneda, J. Sor, Y. Qian, and T. Itoh, "A new quasi-yagi antenna for planar active antenna arrays," *IEEE Transactions on Microwave Theory and Techniques*, vol. 48, no. 6, pp. 910-918, June 2000, doi: 10.1109/22.846717.
- [22] J. I. Lee and J. Yeo, "Modified broadband quasi-Yagi antenna with enhanced gain and bandwidth," *Microwave and Optical Technology Letters*, vol. 55, no.2, pp. 406-409, 2013, doi: 10.1002/mop.27325.
- [23] H. Wang and G. Yang, "Design of 4x4 microstrip Quasi-Yagi beam-steering antenna array operation at 3.5GHz for future 5G vehicle applications," *2017 International Workshop on Antenna Technology: Small Antennas, Innovative Structures, and Applications (iWAT)*, 2017, pp. 331-334, doi: 10.1109/IWAT.2017.7915393.
- [24] S. Poorgholam-Khanjari, F. B. Zarrabi, and S. Jarchi, "Compact and wide-band Quasi Yagi-Uda antenna based on periodic grating ground and coupling method in terahertz regime," *Optik*, vol. 203, p. 163990, 2020, doi: 10.1016/j.jjleo.2019.163990.
- [25] J. Huang and A. C. Densmore, "Microstrip yagi array antenna for mobile satellite vehicle application," *IEEE Transactions on Antennas and Propagation*, vol. 39, no. 7, pp. 1024-1030, July 1991, doi: 10.1109/8.86924.
- [26] S. X. Ta, B. Kim, H. Choo, and I. Park, "Wideband quasi-Yagi antenna fed by microstrip-to-slotline transition," *Microwave and Optical Technology Letters*, vol. 54, no. 1, pp. 150-153, 2012, doi: 10.1002/mop.26504.
- [27] N. O. Parchin *et al.*, "Mobile-phone antenna array with diamond-ring slot elements for 5G massive MIMO systems," *Electronics*, vol. 8, no. 5, p. 521, 2019, doi: 10.3390/electronics8050521.
- [28] S. Saxena, B. K. Kanaujia, S. Dwari, S. Kumar, and R. Tiwari, "A compact dual-polarized MIMO antenna with distinct diversity performance for UWB applications," *IEEE Antennas and Wireless Propagation Letters*, vol. 16, pp. 3096-3099, 2017, doi: 10.1109/LAWP.2017.2762426.
- [29] N. O. Parchin, H. J. Basherlou, Y. I A Al-Yasir, A. M Abdulkhaleq, and R. A Abd-Alhameed, "Ultra-wideband diversity MIMO antenna system for future mobile handsets," *Sensors*, vol. 20, no. 8, p. 2371, 2020, doi: 10.3390/s20082371.
- [30] A. H. Jabire, H. X. Zheng, A. Abdu, and Z. Song, "Characteristic mode analysis and design of wide band MIMO antenna consisting of metamaterial unit cell," *Electronics*, vol. 8, no. 1, p. 68, 2019, doi: 10.3390/electronics8010068.
- [31] W. Jiang, B. Liu, Y. Cui, and W. Hu, "High-isolation eight-element MIMO array for 5G smartphone applications," *IEEE Access*, vol. 7, pp. 34104-34112, 2019, doi: 10.1109/ACCESS.2019.2904647.
- [32] N. M. K. Al-Ani, O. A. S. Al-Ani, M. F. Mosleh, and R. A. Abd-Alhameed, "A design of mimo prototype in c-band frequency for future wireless communications," *Advanced Electromagnetics*, vol. 9, no. 1, pp. 78-84, 2020, doi: 10.7716/aem.v9i1.1333.
- [33] A. S. Abdullah, S. A. Hashem, W. S. Al-Dayyeni, M. F. Mosleh, and I. Hassoun, "Four-port wideband circular polarized MIMO antenna for sub-6 GHz band," *Proceedings of International Conference on Emerging Technologies and Intelligent Systems*, 2022, pp. 909-920, doi: 10.1007/978-3-030-85990-9\_72.
- [34] U. Ahmad *et al.*, "MIMO antenna system with pattern diversity for sub-6 GHz mobile phone applications," *IEEE Access*, vol. 9, pp. 149240-149249, 2021, doi: 10.1109/ACCESS.2021.3125097.
- [35] U. Rafique *et al.*, "Uni-planar MIMO antenna for sub-6 GHz 5G mobile phone applications," *Applied Sciences*, vol. 12, no. 8, p. 3746, 2022, doi: 10.3390/app12083746.





**BIOGRAPHIES OF AUTHORS**

**Haider Saad Najim**     In 2015, he earned a B.Sc. in Computer Engineering Techniques (CET) from the Middle Technical University in Baghdad, Iraq. Since 2017, he has worked as an engineer at the same college's labs. He is presently pursuing an MSc. in Computer Engineering Technology. He is now working on the design and optimization of antennas for 5G mobile networks and other wireless communication systems. He can be contacted by email at: [haidersaadct@mtu.edu.iq](mailto:haidersaadct@mtu.edu.iq).



**Mahmood Farhan Mosleh**     He acquired his B.Sc., M.Sc., and Ph.D. degrees from the University of Technology - Baghdad in 1995, 2000, and 2008, respectively. He worked at Iraq's Middle Technical University as a professor of communication engineering. He has published over a hundred articles in national and international journals. Additionally, attend over 30 International Communication Systems Conferences. He chairs Iraq's Electro-Technical Committee. He authored over 50 articles in a variety of journals in the subject of communications engineering. He can be reached through email at: [drmahfah@yahoo.com](mailto:drmahfah@yahoo.com).



**Raed A. Abd-Alhameed**     In 1982 and 1985, he got B.Sc. and M.Sc. degrees in electrical engineering from Basrah University, respectively, and a Ph.D. degree in 1997 from the Bradford University -United Kingdom. He is presently a University of Bradford Professor of EM and RF engineering. He is now the head of Bradford University's Radio Frequency. He has written approximately 600 academic journal and conference publications in the disciplines of radio frequency, signal processing, propagation, antennas, and electromagnetic computational techniques. He is the principal investigator on several successful EPSRC-funded applications. Since September 2009, he has also served as a research guest at Wrexham University in Wales, focusing on wireless and communications research. He is an Institution of Engineering and Technology Fellow and an Association of Colleges for Higher Education Fellow. He can be reached through email at: [r.a.a.abd@bradford.ac.uk](mailto:r.a.a.abd@bradford.ac.uk).